

# A Chandra HETGS spectral study of the “Big Dipper” 4U 1624-490 and its associated X-ray dust scattering halo

Jingen Xiang<sup>1</sup>, Julia. C. Lee<sup>2</sup> (Harvard University), Michael. A. Nowak<sup>3</sup> (MIT), Jorn Wilms<sup>4</sup> (University of Erlangen-Nuremberg) and Norbert S. Schulz<sup>5</sup> (MIT)

1. jxiang@cfa.harvard.edu 2. jlee@cfa.harvard.edu 3. mnowak@space.mit.edu 4. joern.wilms@sternwarte.uni-erlangen.de 5. nss@space.mit.edu

## Abstract

We present a Chandra HETGS spectral study of the “Big Dipper” 4U 1624-490, and its associated X-ray dust scattering halo. Detailed spectral analysis and associated variability reveal a highly ionized ( $T \sim 3.0 \times 10^6$  K) component associated with an extended accretion disk corona of radius  $R \sim 3 \times 10^{10}$  cm, and a less ionized ( $T \sim 1.0 \times 10^6$  K) variable component coincident with the accretion disk rim, as well as a possible quasi-sinusoidal  $T \sim 43$  ks modulation that we attribute to changes in local obscuration. Based on these studies, a viewing geometry that is mapped to changes in plasma conditions over the 76 ks 4U 1624-490 orbital period is constructed. Further analysis of the associated X-ray dust scattering halo enabled significant improvements on the distance estimate to this source, and a first time determination of non-uniform dust distributions localized to the spirals arms in the Milky Way.

## §1. Introduction

1. Source: 4U 1624-490: A Low Mass X-ray Binary (LMXB), also known as the “Big Dipper” because of its  $\sim 3$  hr dip duration, long orbital period of  $\sim 21$  hr and large obscuration covering  $\sim 90\%$  of the compact object.
2. Dip: Thought to be due to occultations of the central source by gas from the accretions disk rim.
3. Observation: The source was observed with the *Chandra* High Energy Transmission Grating Spectrometer (HETGS) in timed graded mode on 2004 June 4 (ObsID: 4559) for 76 ks, covering one binary orbit (Fig. 1).

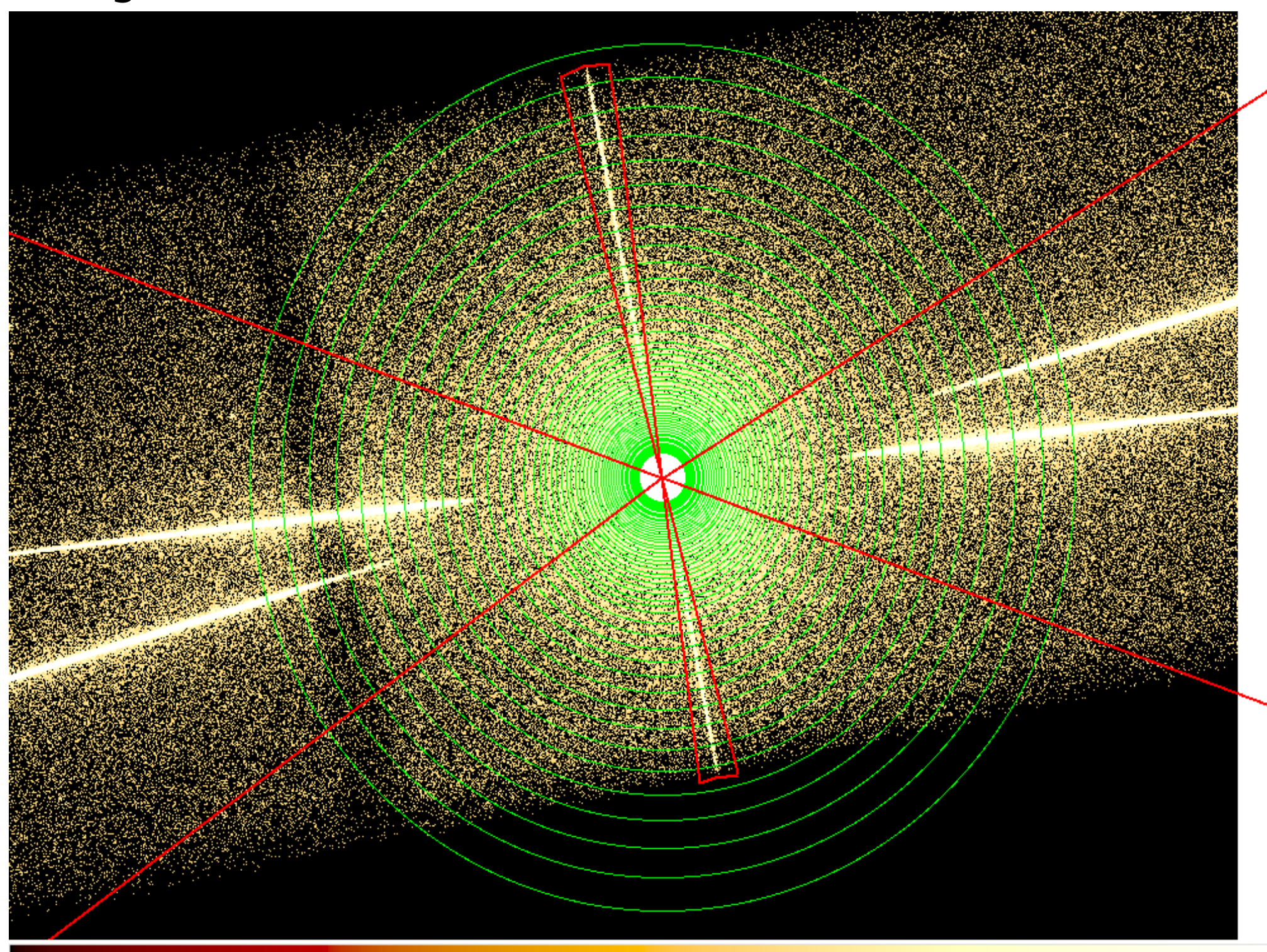


Fig.1 The Chandra HETG/ACIS-S image of 4U 1624-490. The data within the regions marked by the red lines are removed when we extract the halo radial profiles.

## § 2. Scattering Halos

Photons which have been scattered by dust along the LOS travel longer distances than the unscattered one. The delay time  $dt$  is given by

$$dt = 1.15h(D/1kpc)(\theta/1arcmin)^2 \frac{x}{1-x}$$

Therefore the halo and binary light curves can be used to determine the distance to the point source (Fig 2).

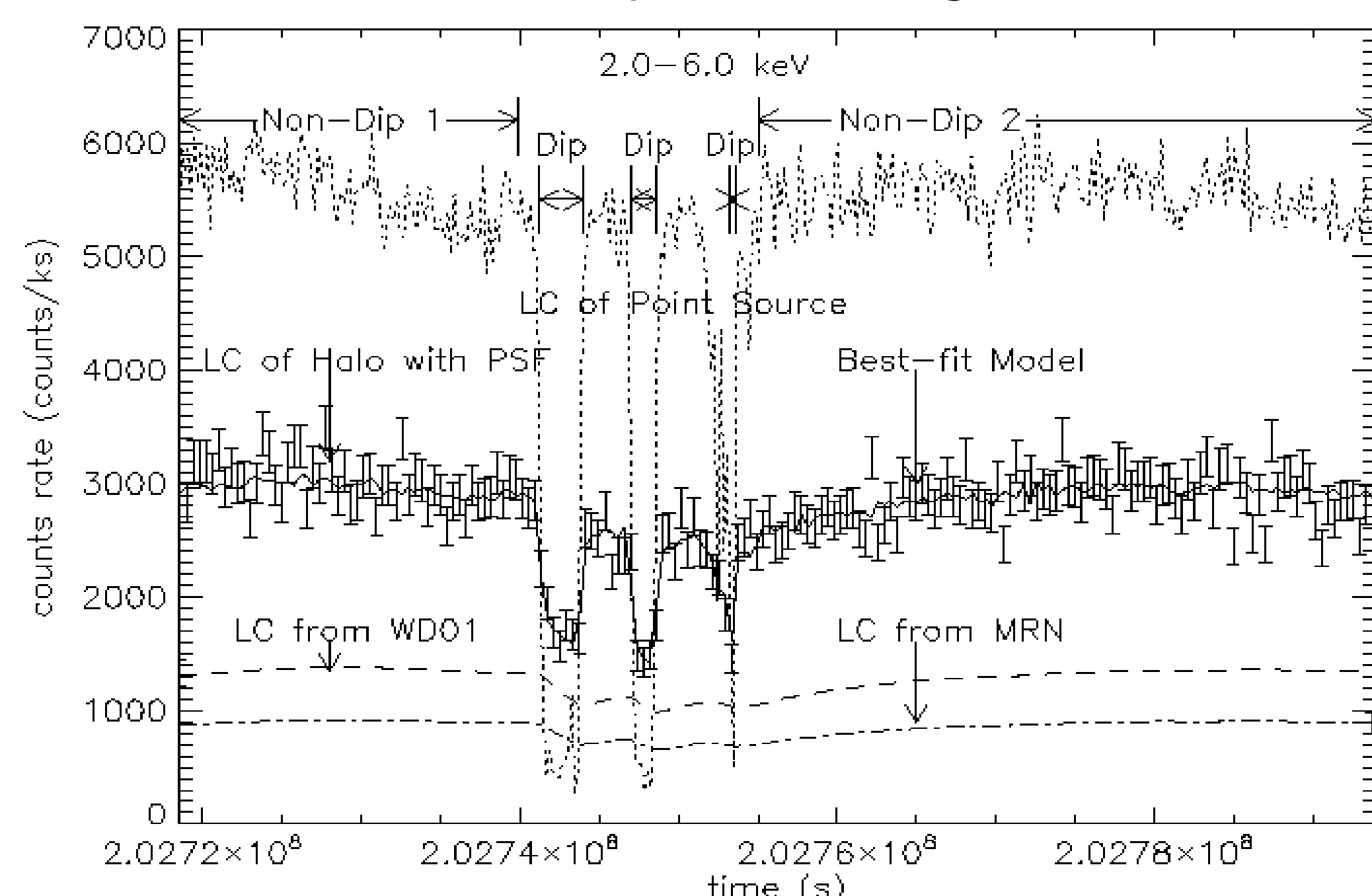


Fig. 2. We derive a distance  $D \sim 15$  kpc from fitting to the light curve of 4U 1624-490 using the dust grain model WD01 [6], assuming uniformly distributed dust.

The observed first order scattering halo intensity  $I_{sca}^{(1)}(\theta, E)$  can be shown as:

$$I_{sca}^{(1)}(\theta, E) = F_x(E) N_H \int_{a_{min}}^{a_{max}} da n(a) \int_0^1 dx f(x) (1-x)^{-2} \times S(a, E, \theta_{sca})$$

So we can determine the spatial distribution of dust from the halo radial profiles. We assume a non-uniform dust distributions along the LOS. Fig. 3 shows the dust distribution along our LOS divided into three parts -- while the dust is assumed to be smoothly distributed in each of these regions, the quantity is allowed to vary independently within a given region.

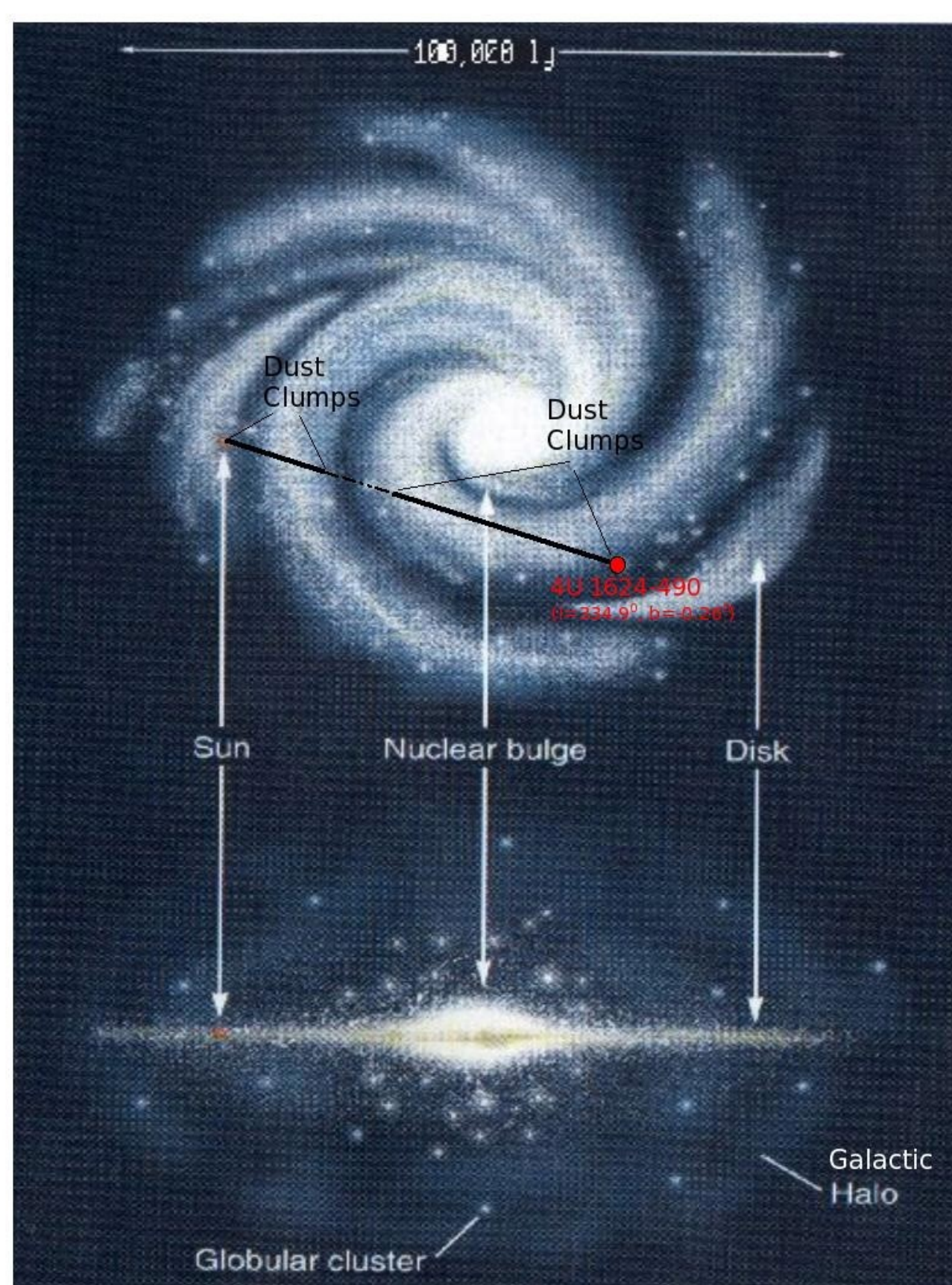


Fig. 3. The location of 4U 1624-490 and the spatial distribution of dust along the LOS.

## § 3. Evolving Broadband Continuum

While the light curves in persistent phase change little over duration of persistent phase (see Fig. 4 (I) seven phases: a, b, ..., and g, each of which lasts  $\sim 10$  ks), the equivalent hydrogen column local to the system changes significantly when a partial covering model is used to fit these broadband continuum spectra (Fig. 4: II and III). The absorbed powerlaw flux changes significantly as well when a blackbody plus powerlaw model is used (Fig. 4: IV and V). Both models indicate that **the observed orbital modulations are predominantly driven by absorption variations.**

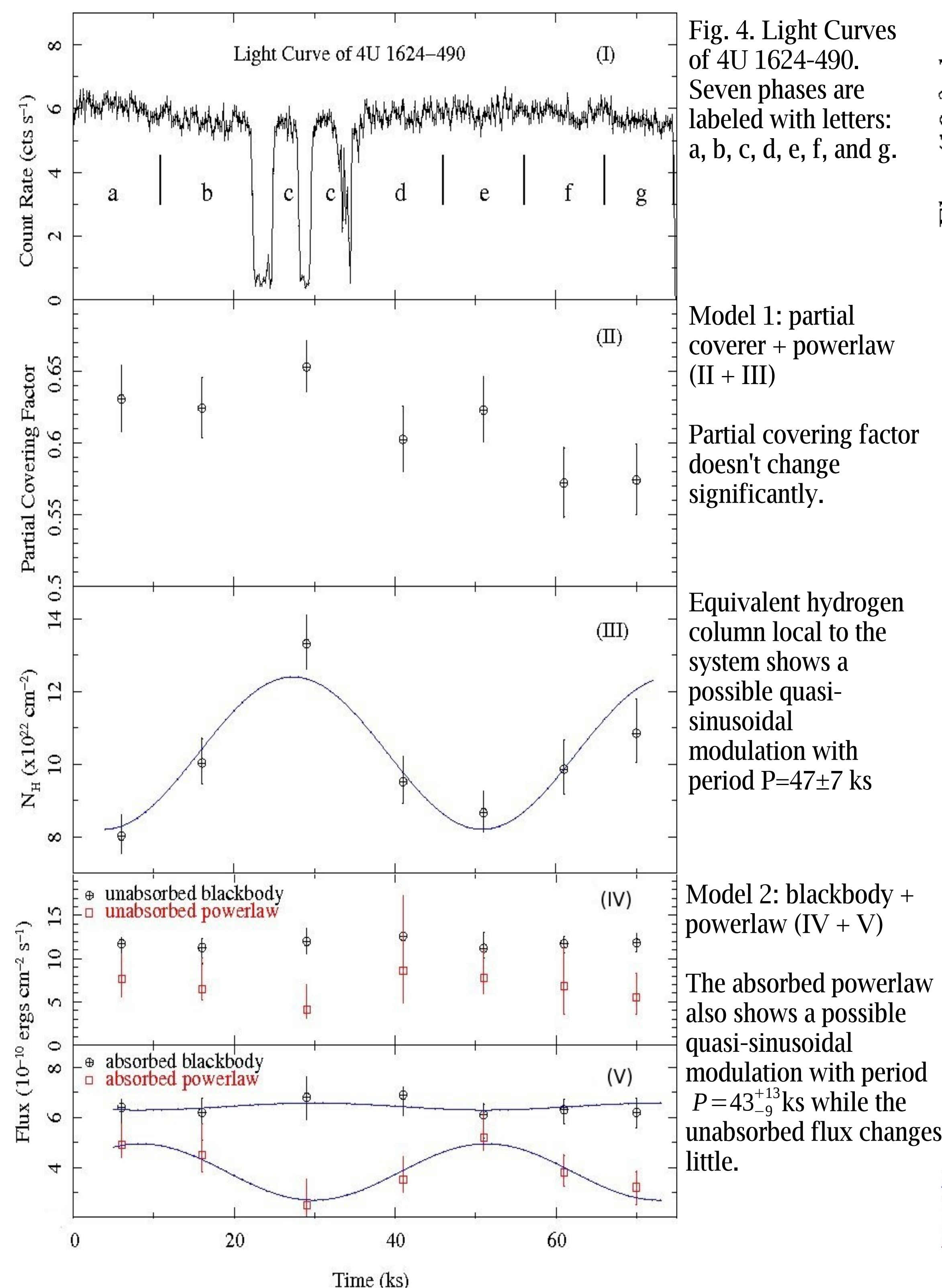


Fig. 4. Light Curves of 4U 1624-490. Seven phases are labeled with letters: a, b, c, d, e, f, and g.

Model 1: partial coverer + powerlaw (II + III)  
Partial covering factor doesn't change significantly.

Equivalent hydrogen column local to the system shows a possible quasi-sinusoidal modulation with period  $P = 47 \pm 7$  ks

Model 2: blackbody + powerlaw (IV + V)  
The absorbed powerlaw also shows a possible quasi-sinusoidal modulation with period  $P = 43_{-9}^{+13}$  ks while the unabsorbed flux changes little.

## § 4. Evolving Line Profiles with Phase

The ionized H-like and He-like Fe lines also show variability in both flux and wavelength (Fig. 5 and 6). The green lines indicate the laboratory wavelengths of Fe XXV (1.850 Å) and Fe XXVI (1.778 Å) resonant absorption.

As a first step, we assess spectral changes during phases far from the dip ( $a+e+f+g$ ) and those immediately before and after ( $b+c+d$ ) it by analyzing data which have been divided into these two categories.

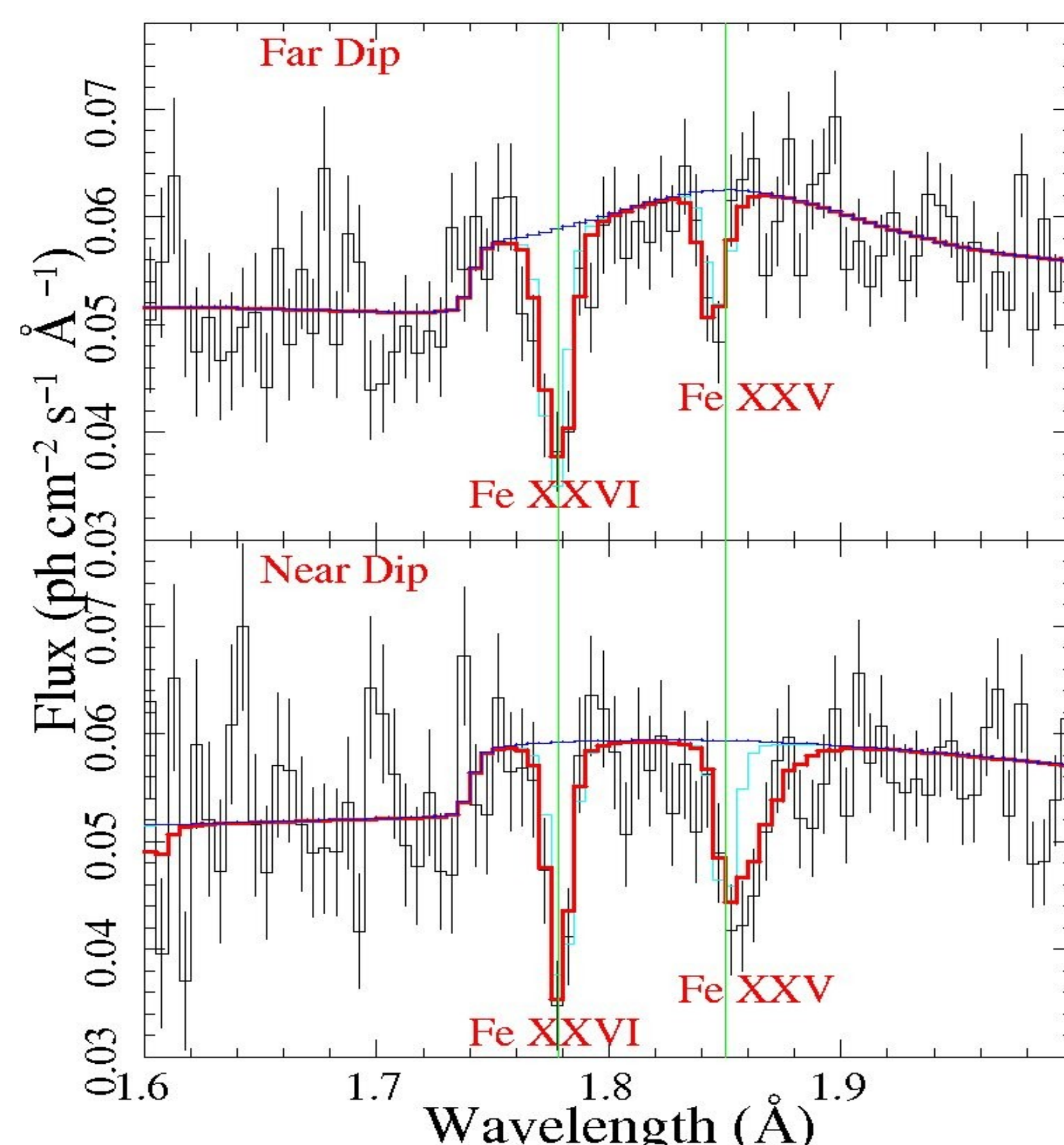


Fig.5. Best fit ionized absorber models (red) and the insufficient single absorber models (light blue) overplotted on the HEG 1<sup>st</sup> order far dip (top) and near dip (bottom) spectra.

A single absorber for fitting either of these spectra is not sufficient. Therefore, we use **a dual absorber (one hot at  $T \sim 3 \times 10^6$  K and one less so  $T \sim 10^6$  K) to fully describe the observed lines.**

Using the relation between ionization parameter and the radius of plasma gas, we estimate the radius of  $\sim 3 \times 10^{10}$  cm for the hot gas, which is consistent with the location of the Accretion Disk Corona (ADC) in 4U 1624-490 as determined by *Church et al 2004*. Similarly the  $\sim 10^{11}$  cm radius of less ionized gas is consistent with the truncation radius of the disk. Fig. 7 shows the location of these absorbers in the context of 4U 1624-490 geometry.

We also divided the persistent spectrum into 7 parts of  $\sim 10$  ksec duration (Fig. 6). The Fe XXV and Fe XXVI line fluxes and profiles clearly evolve with phase.

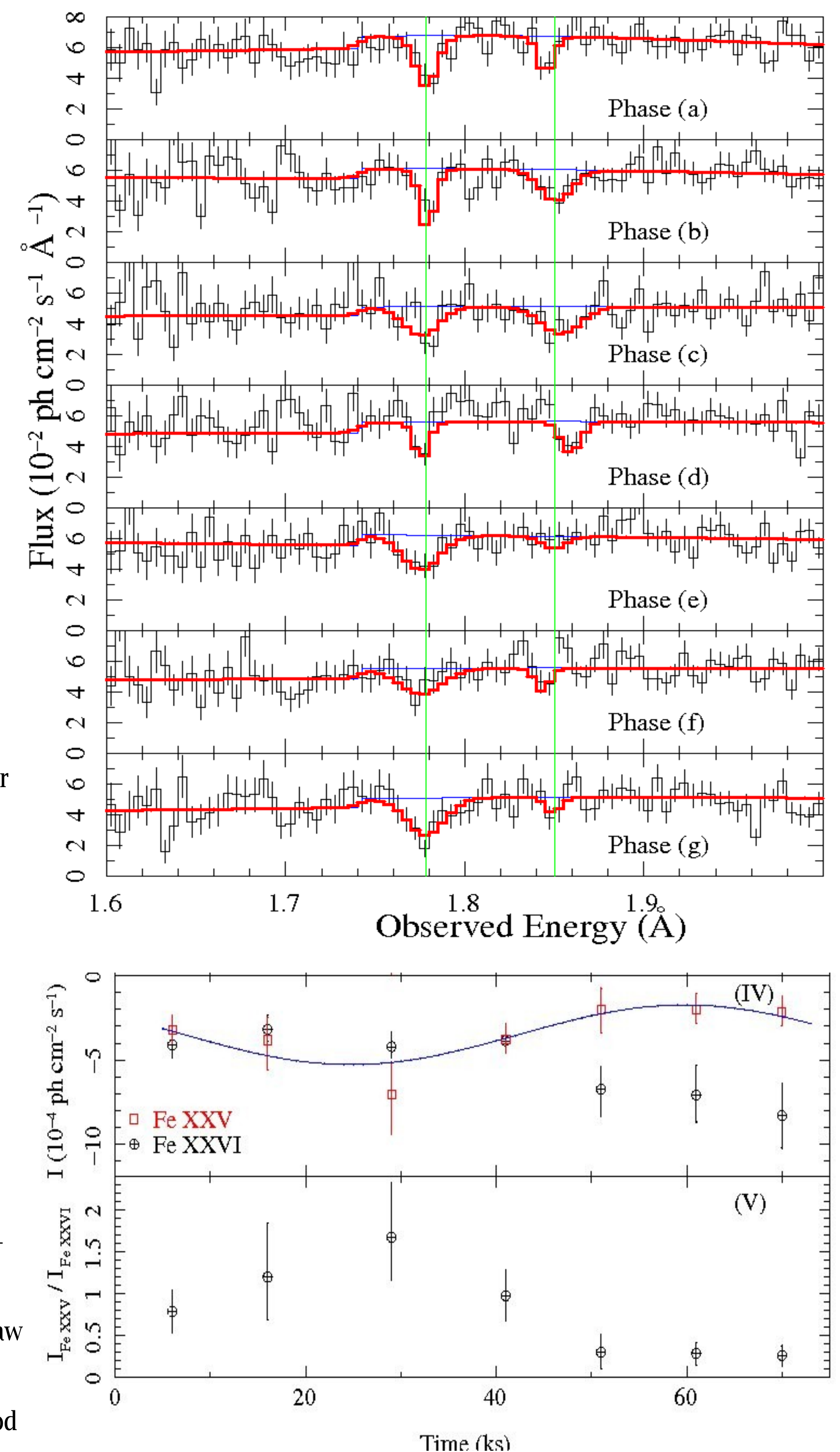


Fig. 6. The evolution of Fe XXV and Fe XXVI lines

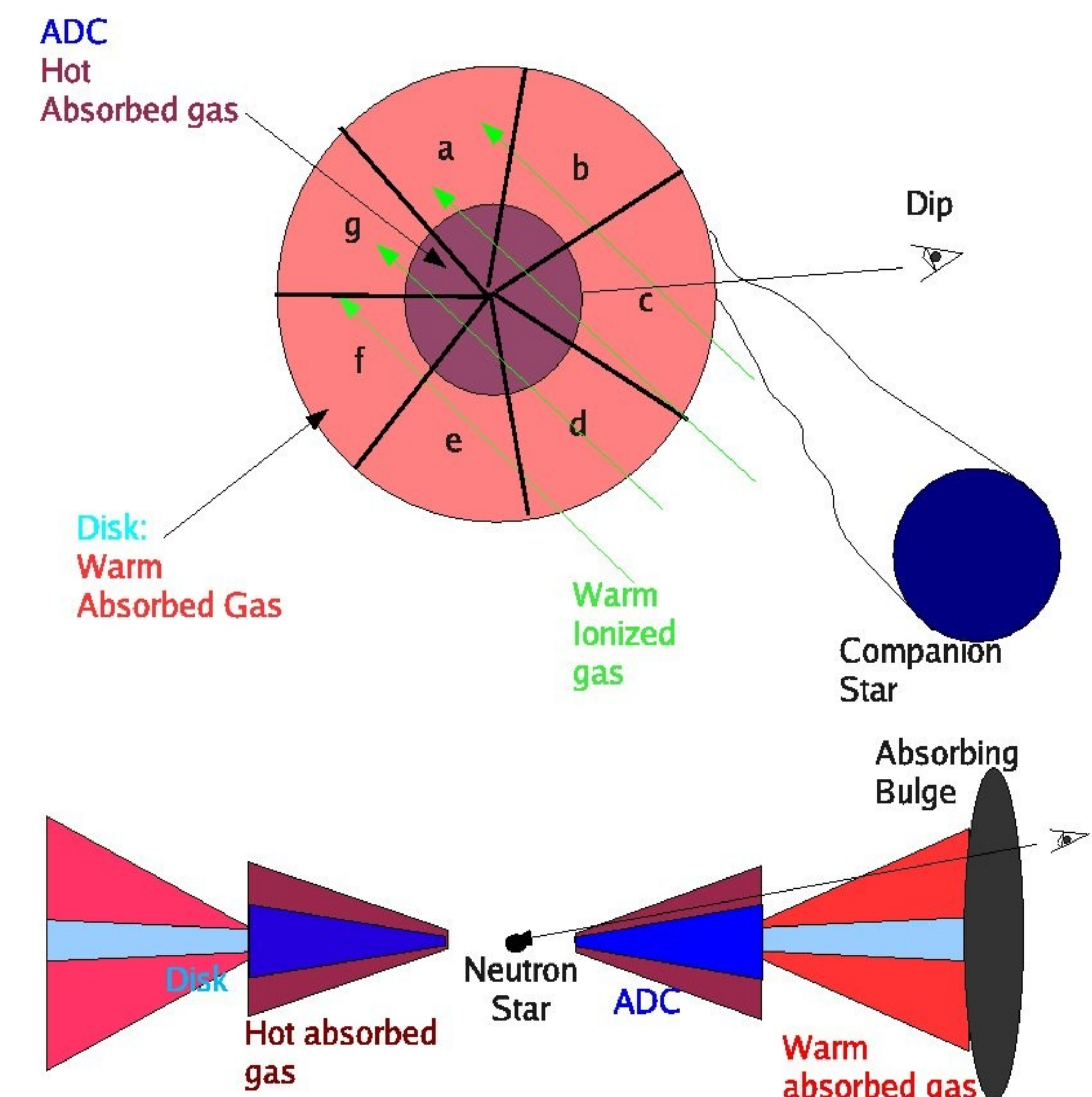


Fig. 7 Geometry of 4U 1624-490 showing the location of the two temperature ionized gas as it evolves with phase.

## Conclusions:

### (1) Xiang, Lee & Nowak 2007:

- We determine a distance  $D_{4U1624-490} = 15.0_{-2.6}^{+2.9}$  kpc to 4U 1624-490 based on scattering halo studies.
- Varying dust distribution **does** affect the derived column densities along the LOS to 4U 1624-490. A simple estimate based on our halo fits imply the hydrogen particle density in the spiral arms is  $n \sim 1.6$   $\text{cm}^{-3}$  and the one between two spiral arms  $n < 0.3$   $\text{cm}^{-3}$ .

### (2) Xiang, Lee, Nowak, Wilms & Schulz 2009:

- A possible quasi-sinusoidal modulation with period  $P = 43_{-9}^{+13}$  ks, are predominantly driven by changes in obscuration, rather than any intrinsic variation of the power-law or black-body components.
- Evolving iron absorption line profiles with orbital phase during the persistent phase of 4U 1624-490 are observed.
- The evolution of these lines can be modeled using the “XSTAR” photoionization code which places the location of the gas in the region of the ADC and disk.

## Main References:

- [1]. Caswell J. L. & Haynes F. F. 1987, A&A, 171, 261
- [2]. Church M., J. & Balucinska-Church, M. 2004, MNRAS, 348, 955
- [3]. Mathis, J. S., Rumpf, W. & Nordsieck, K. H. 1977, ApJ, 217, 425 (MRN)
- [4]. Mathis, J. S. & Lee, C. W. 1991, ApJ, 376, 490
- [5]. Predehl, P., Burwitz, V., Paerels, F., & Trümper, J. 2000, A&A, 357, L25
- [6]. Weingartner, J. C. & Draine, B. T. 2001, ApJ, 548, 296 (WD01)
- [7]. Xiang, J., Lee J. C., & Nowak, M. A., 2007, ApJ, 660, 1309
- [8]. Xiang, J., Lee J. C., Nowak, M. A., Wilms, J., & Schulz N. S., 2009, ApJ, 701, 984